Superconducting self-balancing system for vehicle suspension and guide

Gino D'Ovidio, Francesco Crisi and Giovanni Lanzara
University of L'Aquila, Faculty of Engineering, DAU, Via G. Cronchi 18, 67100 L'Aquila, Italy
gino.dovidio@univaq.it

ABSTRACT: This article examines the lifting and guiding performances of an experimental self-balancing "V" shaped superconducting levitated module for UAQ4 train the feasibility of which has been successfully tested in laboratory. The work concept of maglev module is based on pinning effect of YBCO bulk superconductors mounted on board of vehicle that interacts with the magnetic field of permanent magnets distributed on the guide-way. It is 100% magnetic resistance free motion. The performances of the maglev module are evaluated by varying the system parameters of a finite element numerical model refined with experimental data. The results of levitation tests and numerical analysis are presented and discussed.

1 INTRODUCTION

At the Transportation Laboratory of the University of L'Aquila the main components of UAQ4 levitating train technologies have been defined and comprehensively tested.
The system is a guided train using superconductors and permanent magnets for lifting and guiding.
Pinning phenomena of the magnetic flux determines the levitation in a stable equilibrium and self-balancing state when the high temperature bulk superconductor (HTS) interacts with the magnetic field of the permanent magnet (PM).
Other authors [1-4] have already proposed and tested demonstrator transport systems using onboard HTS equipment that interacts with guide-ways employing PM assembled in opposite dipole symmetry, separated and sided by flux concentrators of steel giving rise to a gradient field vertically to generate lift force; lateral (guidance) force is only dependent on the trapped flux in the HTS bulk sample. Maglev vehicles are currently driven by a traditional alternate current (AC) linear motor.
With respect to the current technical state of art we have introduced two novel aspects [5-6]:

a) A "V" shaped self-balancing, magnetically-levitated module generating both stable lift and guidance [5-6];
b) Propulsion provided by a direct current stepper linear motor [7].

The maglev module is both self-stabilizing and magnetic drag free to the motion. It is conceived to create a gradient field on the topside and to increase, at same time, the guidance force by adding a lateral repulsive force to one of the trapped flux in the superconductors.
The propulsion system uses the PM of the central beam as the stator and the on-board coil power supplied as the rotor instead of current inductive or synchronous alternate current (AC) linear motors.
UAQ4 is a magnetic levitating vehicle with 100% magnetic resistance free motion. The system significantly minimizes the consumption and the environmental impact as it does not have any vibrations, noise or pollution.
UAQ4 train can operate at both low speed in urban environment and at high speed for long distance trips.
This article is focused on the study of the experimental maglev module by performing both experimental and numerical analyses.

2 SET UP AND TESTS

To test the maglev system performance, a simplified set up reproducing the magnetic behavior of a UAQ4 maglev module was designed and constructed.
The basic work principles of the maglev module is based on the levitation force behavior of HT superconductor. As well know, pinning of the magnetic flux determines the levitation of the type II superconductor in a stable equilibrium state when the

sample is levitating above or suspended below the PM.

Let a bulk superconductor disk shaped be suspended below a PM at distance, where the magnetic flux density is *B*; the magnet field is perpendicular to the disk plane and *Z*-axis is directed vertically and coincides with the disk axis. For this system, the weight of superconductor disk is balanced by the levitation force which can be calculated using the well known equation:

$$F_Z = Jc \cdot d \cdot (\partial B/\partial Z) \qquad (1)$$

where *Jc* is critical current density, d is the perimeter of induced shielding current loops, and ∂B/∂Z is the gradient of magnet field.

The levitation force is also influenced by the shape and thickness of the bulk superconductor, field cooling process and operating temperature.

In accordance with the theory, the levitation module uses PM assembled in a "V" shaped iron beam, the static magnetic field of which interacts with the HTS runner that has the same shape.

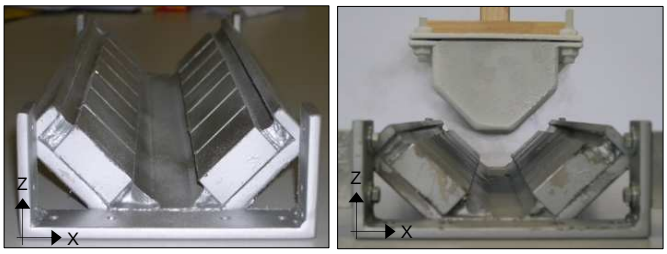

a) b)

Figure. 1. Set up: iron magnetic guideway without a) and with b) HTS runner cooled @ 77K

Figure 1 shows the set up, the main components of which are:

a) A magnetic guideway section that includes an iron beam with NeFeB permanent magnets arranged in a *Y* direction (along the movement of the vehicle) and two homopolar arrays facing each other, of opposite polarization along the transversal direction *X* (Fig. 1a) ;
b) A simplified HTS runner device consists of "V" assembled close arrays of melt textured YBCO monoliths, immersed in liquid nitrogen kept at low temperature in a suitable cryogenic vessel with non magnetic steel walls (Fig. 1b) .

The set up functioning is based on the interaction between the cooled HTS runner and magnetic field of PM of the beam section. The HTS runner is mounted above the magnetic beam by means of a hydraulic jack, joined to a precision mechanical device, permitting variation in the operational gaps between the two components. The levitation forces were tested on the HTS runner using a measurement system consisting of a bi-axial sensor.

The experimental magnetic beam section is 380 mm long and uses NeFeB permanent magnets with dimensions of 50x40x18mm.

The experimental HTS runner of 190 mm uses melt textured YBCO samples (thickness of 11mm) that are fixed in a cryogenic vessel (5 mm thickness multi-layers wall) filled with liquid nitrogen.

The main geometrical data of set up are listed in Tab. 1 according to the symbols of Figure 2.

Tab1. Dimensions of experimental levitated module

α	a	b	c	d	e	f	L	H
(deg)	(mm)	(mm)	(mm)	(mm)	(mm)	(mm)	(mm)	(mm)
45	40	18	31	8	6	10	147	60

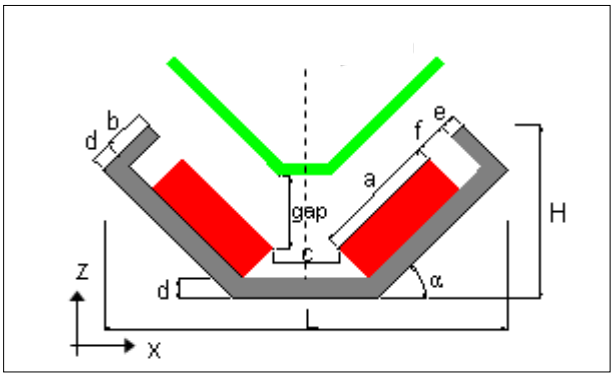

Figure 2. Cross section scheme of maglev module

At first, the magnetic field of guide-way was tested by using an hall probe; the results of magnetic field characterization are shown in Figure 3 as vectorial representation of flux density. The magnetic flux is confined inside the iron structure and it is summed in air; the iron works as collector of magnetic field in the bottom side.

Several levitation tests in semi-static condition were performed by using the experimental set-up described above and by cooling the YBCO structure in a zero magnetic field with liquid nitrogen.

It was verified that this maglev module floats with a large air-gap and that no control devices are required to keep the gap constant and no drag force is generated during the motion along *Y* direction [8-12].

Figure 4 shows the levitation forces vs. gap tested by the experimental set-up.

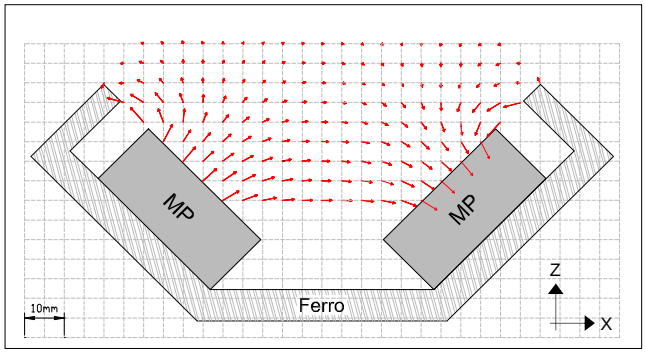

Figure 3. Vectorial representation of flux density

To compare the levitation results obtainable by different module sizes, we introduced a specific lift force F_Z (N/m) and guidance force F_X (N/m) defined as the lift and guidance forces per one meter of maglev module, respectively.

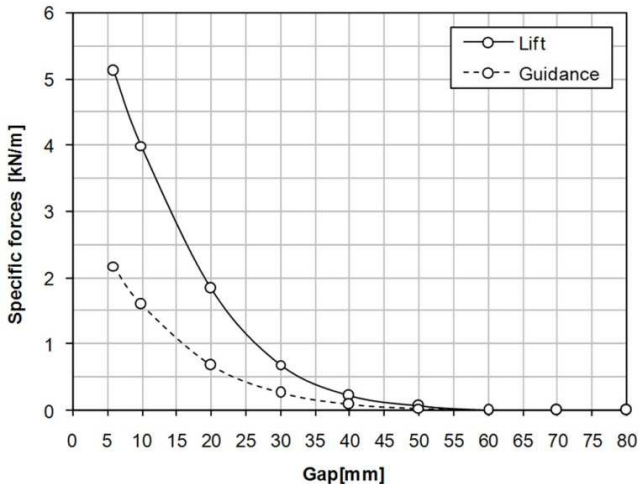

Figure 4. Levitation performances vs. gap (experimental maglev module)

One can see that significant levitation magnitudes at high gap values are achieved. The levitation thrusts stably increases with decreasing gap; moreover the ratio between F_X and F_Z is fully adequate to mass transportation application requirements.

3 NUMERICAL ANALYSIS

The performance of the proposed maglev module was also evaluated by using a 2D and 3D finite element (FE) parametric model.

A good agreement between experimental and numerical data were obtained by taking into account the following parameters: rare-earth magnets (Br =1.2T, HC=-1270kA/m, μ_r=1), non-linear B-H characteristics for the massive iron and a low electrical resistivity (10^{-10} Ωm), relative permeability value equal to 1 for modeling the superconducting material.

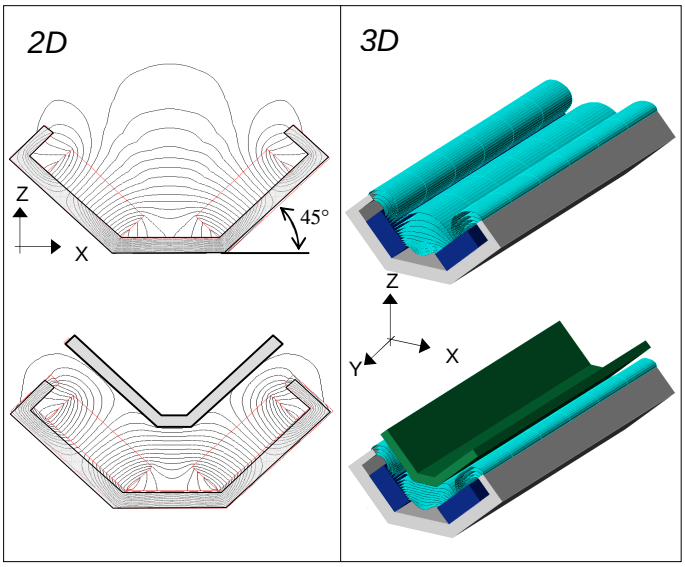

Figure 5. Numerical analysis: 2D and 3D guideway flux density configurations without and with HTS runner

Figure 5 shows 2D and 3D views of flux density for two system configurations without and with the HTS runner, respectively.

The maglev module has been analyzed in the Z-X plane by calculating the system magnetic reactions given rise in opposition to external actions (F_X, F_Y, M_Y) put on the HTS runner. The external actions are introduced as combination of vertical ($v_Z = \partial u_Z/\partial t$), horizontal ($v_X = \partial u_X/\partial t$) and rotational ($\omega_Y = \partial \varphi_Y/\partial t$) speeds for two different starting angle (φ_0) configurations.

The following values for HTS runner are taken into account:

- $\varphi_0 = 0$ (HTS runner is centered on the guideway);
- $\varphi_0 = 18°$ (HTS runner is rotated on the guideway).
- $v_Z = 0$ and 0.03 m/s
- $v_X = 0$ and 0.03 m/s
- $\omega_Y = 0$ and 0.15 Hz

where u_z and u_x are the vertical and the horizontal displacement, ω_Y is the rotation.

Figure 6 shows maglev module reactions due to combination of vertical (v_Z) and rotational (ω_Y) speeds for φ_0=0 and φ_0=18° respectively.

The results show that the maglev module is self stabilizing and self balancing since the external actions are contrasted by internal magnetic reactions tending to move the HTS runner in the centered

position since it correspond the minimal energetic level of system.

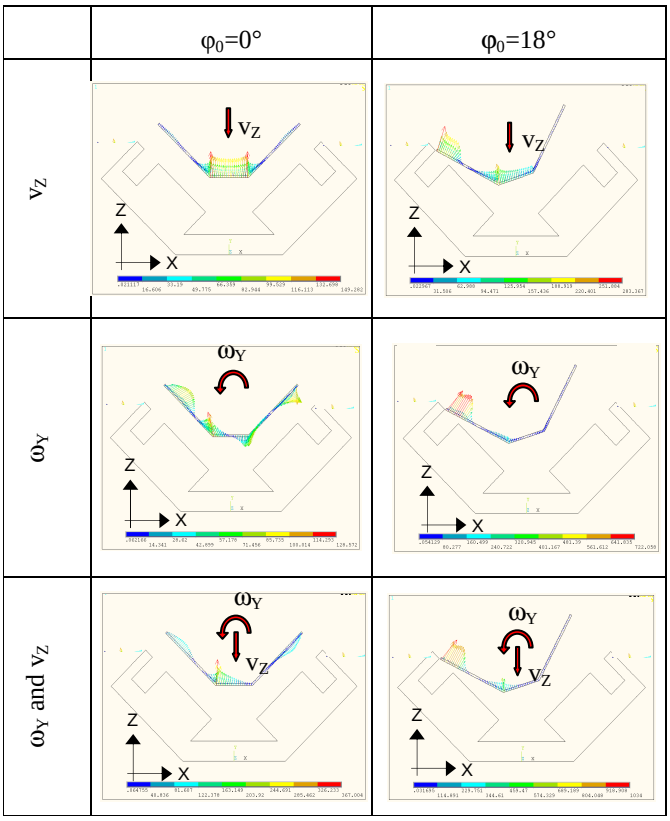

Figure 6. Maglev module reactions due to combination of vertical (v_Z) and rotational (ω_Y) speeds for two starting angle (φ_0) system configurations

Figures 7, 8 and 9 show the module reactions (lift force, guide force and torque) Vs. system starting angle (φ_0) at a combination of four external speed components as following:

a) $v_X + v_Y$
b) $v_X + \omega_Y$
c) $v_Z + \omega_Y$
d) $v_X + v_Z + \omega_Y$

The results show that the system instantaneously reacts to external actions by generating internal reactions in terms of lift forces, guide forces and torques. The internal work of maglev module is unaffected by energy losses and consequently no drag forces are produced.

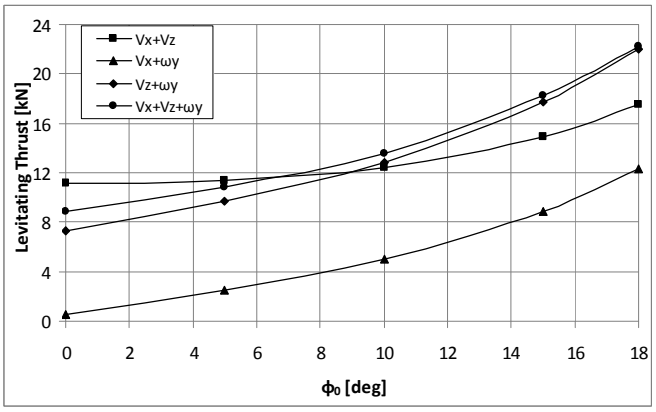

Fig. 7 Lift thrust Vs. starting angle (φ_0) system for speed components combination

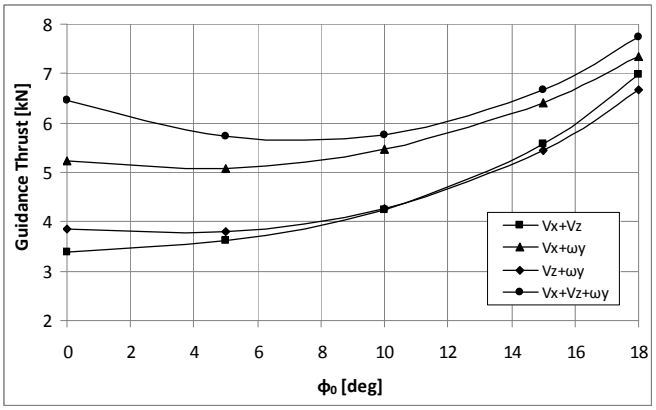

Fig. 8 Guidance thrust Vs. starting angle (φ_0) system for speed components combination

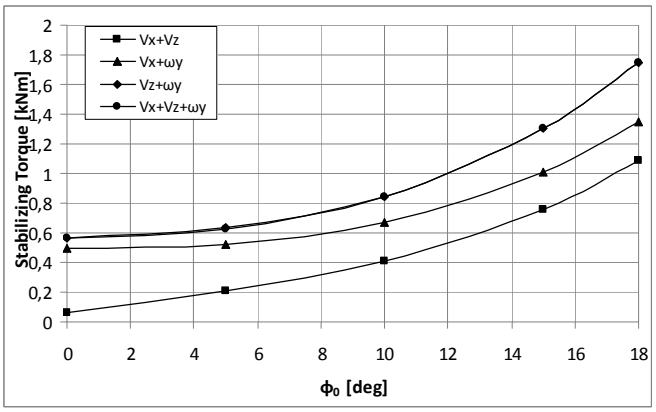

Fig. 9 Stabilizing torque Vs. starting angle φ_0 system for speed components combination

4 CONCLUSIONS

The basic work principles of a novel "V" shaped maglev module is presented and discussed. It is based on the self-balancing levitation force behavior of

YBCO bulk superconductor interacting with magnetic field of permanent magnet.
The lifting and guiding performances of the maglev module have been verified by several levitation tests in semi-static conditions.
It was verified that proposed maglev module floats with a large air-gap and that no control devices are required to keep the gap constant and no drag force is generated during the motion.
Moreover the maglev module performances were analyzed by finite element parametric model refined with experimental model and by varying the system parameters. The analysis results have highlighted the self balancing behavior of maglev module when it is stressed by external actions or moments.

5 REFERENCES

[1] J. Wang, S. Wang, et al., Journal of Physica C 378–381 (2002) 809.
[2] J. Wang, S. Wang, et al., Superconductor Science and Technology 18 (2005) S215.
[3] O. de Haas, L. Schultz, P., et al. in: 18th International Conference on Magnetically Levitated Systems and Linear Drives, Shanghai, China, 2004, 326.
[4] L. Schultz et al., IEEE Trans. Appl. Supercond. 15 (2) (2005) 2310.
[5] G. Lanzara US patent n. 4,797,445
[6] G.Lanzara, G. D'Ovidio. F. Crisi, Italian Patent 0001386002 (2007)
[7] G. D'Ovidio, G. Lanzara, F. Crisi, Italian patent 0001385998 (2007)
[8] G. D'Ovidio G., F. Crisi, G. Lanzara Journal of Optoelectronics and Advanced Materials pp 1011-1016 (2008) Vol.10, Issue 5
[9] G. D'Ovidio, G. Lanzara, F. Crisi Journal of Physica C 1036-1040 (2008) 468
[10] G. D'Ovidio, F. Crisi, A. Navarra, G. Lanzara, IEEE J. Trans. Ind. Appl. 126 (10) (2006) 1336.
[11] G. D'Ovidio, F. Crisi, A. Navarra, G. Lanzara, Journal of Physica C 449 (2006) 15.
[12] G. D'Ovidio, F. Crisi, A. Navarra, G. Lanzara, Journal of Mater. Process. Technol. 181 (1–3) (2007) 18.